

# Generalization of Impedance Characterization Methods for Liquid Crystal-Embedded Tunable Transmission Lines and Applied Study into Guard Band Redundancy Evaluation

Jinfeng Li, *Member, IAENG*, Haorong Li, Yunchen Xiao, Peixin Jiang, Sibowang, and Zehan Guo

**Abstract**—In the trajectory of millimeter-wave (mmW) reconfigurable components advancement leveraging liquid crystals (LCs), a comprehensive array of planar and non-planar transmission lines, along with their diverse iterations, has emerged over the past two decades. This study introduces a unified framework for impedance characterization and benchmarking employing three distinct methodologies, i.e.,  $Z_{pi}$  (power-current),  $Z_{vi}$  (voltage-current), and  $Z_{pv}$  (power voltage). These frameworks are applied to three types of phase-variable transmission lines, namely, inverted microstrip line (IMSL), strip line (SL), and coaxial line (CL), each integrated with highly anisotropic nematic LCs as electronically tunable mediums. While these three topologies feature dual conductors, their fundamental disparity lies in the presence or absence of non-tunable dielectrics, thus influencing the interaction of mmW power with the transmission lines. Computational benchmarking at 60 GHz affirms the phenomenon of  $Z_{pi} > Z_{vi} > Z_{pv}$  across the three topologies, albeit with varying degrees of deviation contingent upon geometric aspect ratios of the core line width to the LC layer thickness, as well as the permittivity ratio between tunable (LC) and non-tunable dielectrics (specifically pertinent to IMSL). Notably, aiming for 50  $\Omega$  at 60 GHz and with identical LC permittivity, the maximum deviation among the three impedances is 2.496  $\Omega$  for the IMSL, followed by 2.015  $\Omega$  for the strip line, and a minimal 0.254  $\Omega$  for the coaxial counterpart. Arguably, the deviations reduce with the enhancement of shielding towards a true TEM mode. Based on the impedance characterizations, a conservativeness assessment of TE<sub>11</sub> cutoff guard band allowance for 300 GHz LC-filled coaxial phase shifters is conducted. Extending the implications of these findings, such a nuanced understanding of impedance characteristics and deviation patterns is instrumental in optimizing the design and performance of mmW reconfigurable

components utilizing LC-based transmission lines towards enhanced adaptability and performance in diverse applications such as 5G/6G wireless communication networks, radar systems, and beyond.

**Index Terms**—characteristic impedance, coaxial, delay line, inverted microstrip, liquid crystal, millimeter-wave, phase shifter, strip line, terahertz, 60 GHz

## I. INTRODUCTION

NEMATIC liquid crystal [1] is well-recognized as a functionally anisotropic dielectric material (molecules in nanoscale), featuring an electronically (or magnetically) variable electric permittivity (dielectric constant in the macroscopic scale) that can be leveraged for electromagnetic (EM) wave speed control (i.e., phase shifting or time delaying of an EM wave signal), and hence the wavefront manipulation (e.g., beamforming and beam steering) if grouping the various phase-shifted radiators in an array [2]. The underpinning components enabled by the nematic liquid crystal for realizing these wavefront (beam) reconfigurability are arguably phase shifters.

The full-stack developments of nematic liquid crystal (abbreviated as LC)-enabled dielectric-tunable transmission line phase shifter devices have been evidenced in our pilot works reported in [1][2], targeting 54 GHz to 66 GHz beam-steering applications, e.g., WiGig (Wireless Gigabit) [3], and intelligent reconfigurable surfaces (IRS) [4], albeit tremendous challenges remain for global commercialization at a reasonable cost whilst upholding undegraded performance (e.g., the phase-shifting precision, the phase-controlling stability or uncertainty, the response speed, the temperature stability or reliability, the insertion loss predictability, the mixed-signal integrity, among many others [5]).

Various complementary techniques [5] have been implemented afterwards to upgrade the relevant device's figure-of-merit [6], minimize the insertion loss imbalance [7] (amidst diverse tuning states of LCs by applying different amplitudes of the voltage), reduce the footprint (by meandering the shielded coplanar waveguide [8]), and so on, in addition to many fundamental science contributions [9] from the foundational electromagnetic science parlance to the betterment of the overall application system performance. Specifically, we identified three different types of characteristic impedance ( $Z$ ) characterizing methods (i.e.,

Manuscript received September 8, 2024; revised December 18, 2024.

This work was supported in part by the National Natural Science Foundation of China (under Grant 62301043), and in part by the Fundamental Research Funds for the Central Universities (Beijing Institute of Technology Research Fund Program for Young Scholars) under grant number 220502052024011.

Jinfeng Li is an assistant professor at the Beijing Key Laboratory of Millimeter Wave and Terahertz Technology, School of Integrated Circuits and Electronics, Beijing Institute of Technology, Beijing, 100081, China (corresponding author, e-mail: jinfengcambridge@bit.edu.cn).

Haorong Li is a postgraduate student at Beijing Institute of Technology, Beijing, 100081, China (email: haorong.li@bit.edu.cn).

Yunchen Xiao is an undergraduate student at Beijing Institute of Technology, Beijing, 100081, China (email: xiaoyunchen@bit.edu.cn).

Peixin Jiang is an undergraduate student at Beijing Institute of Technology, Beijing, 100081, China (email: jiangpeixin@bit.edu.cn).

Sibowang is an undergraduate student at Beijing Institute of Technology, Beijing, 100081, China (email: huangsibowang@bit.edu.cn).

Zehan Guo is an undergraduate student at Beijing Institute of Technology, Beijing, 100081, China (email: gzh@bit.edu.cn).

power-current, power-voltage, and voltage-current) when studying the behavior of  $Z$  versus  $T_{LC}$  (the LC thickness) for LC-filled coaxial phase shifters at the unlicensed 60 GHz band [10], wherein we concluded that the power-current and voltage-current methods closely agree (with each other), while the power-voltage technique shows a lower estimate by simulation (albeit the deviation is less than  $0.4 \Omega$  for the coaxial situation [10]).

There is, however, to the best of our knowledge, a lack of cross-referencing or generalization to the mainstream planar transmission line structures, e.g., strip lines (SL) [11][12], microstrip lines [13][14][15], and more specifically, inverted microstrip lines (IMSL) [16][17] that suits the LC accommodating purpose.

To this end, this work explicitly bridges this gap by compiling the up-to-date results of the planar (IMSL and SL) ones (besides those from the non-planar coaxial ones that have already reported [6][10]) and verify the applicability of the three characteristic impedance ( $Z$ ) characterization approaches (power-current, power-voltage, and voltage-current), i.e., we seek to understand the deviations encountered amidst the  $Z$  results that diverse characterizing methodologies deliver, and if the implications apply to all the transmission lines as mentioned above.

This paper is decomposed into two main parts. Section II comparatively studies (by simulation) the characteristic impedance characterization of SL, IMSL, and coaxial delay lines (all based on the LC-combined technology) with three distinct computationally-measuring approaches (numerically simulated and benchmarked with theoretically derived results at 60 GHz by way of illustration). Based on the insights and conclusions drawn from section II (informing the LC-based phase shifter device design at an early stage of the device's geometry regulation, i.e., as per the  $50 \Omega$  standard of impedance matching), section III follows as an applied study into one of the three transmission line topologies (i.e., the LC-filled coaxial delay line) for achieving a variable phase shifter. More specifically, we advance the existing design knowledge from 60 GHz to 300 GHz (i.e., 0.3 THz), wherein a guard band allowance (by percentage) is defined and evaluated to keep away from the higher-order-mode cutoff conservatively.

## II. METHODS AND RESULTS

With a dedicated finite-element method (FEM) based full-wave electromagnetic (EM) solver, the input wave port impedances ( $Z$ ) of the LC-filled phase shifting devices are computed at 60 GHz in the aforementioned three characterization paradigms, i.e., power-current ( $Z_{pi}$ ), power-voltage ( $Z_{pv}$ ), and voltage-current ( $Z_{vi}$ ), for three geometry types of IMSL, SL, and coaxial phase shifters, all filled with the nematic LCs of the similar material grade [18][19][20], i.e., with a dielectric constant ( $Dk$ ) of 3.3 at the maximally achievable dipole moment state. Readers interested in delving into the mechanism of the variable dipole moment of LCs can refer to [1] for more physics and mathematics.

The formulas for the three calculation paradigms are mathematically summarized and described by (1)(2)(3) below, respectively, while the analytical expression (TEM-mode assumed) for the coaxial topology [6] is

governed by (4), wherein  $Dk_{eff}$  represents the effective dielectric constant ( $Dk$ ) of the medium (media) surrounding the wave-guiding conductors for a transmission line or a waveguide,  $T_{LC}$  represents not only the filled LC thickness for the tunable dielectric layer sandwiched, but also the spatial distance between the core and ground conductors, and  $D_{core}$  indicates the diameter of the core conductor.

$$Z_{pi} = \frac{P}{I^2} \quad (1)$$

$$Z_{pv} = \frac{V^2}{P} \quad (2)$$

$$Z_{vi} = \frac{V}{I} \quad (3)$$

$$Z_0 = \frac{60}{\sqrt{Dk_{eff}}} \ln\left(1 + 2 \frac{T_{LC}}{D_{core}}\right) \quad (4)$$

For the IMSL and SL phase shifters, the filled dielectric thickness (i.e., the nematic LC thickness of  $T_{LC}$ ) is fixed at 0.1 mm for a decent trade-off between the tuning speed and the insertion loss. Note that the trade-off competition here has yet to constitute a geometry optimization that is being conducted. Based on the assumption of  $T_{LC}=0.1$  mm, a parametrization against the core line width ( $W_{core}$ ) is carried out.

Since voltage is not uniquely defined for quasi-TEM structures, the computational results of the  $Z_{pv}$ ,  $Z_{vi}$ , and  $Z_{pi}$  are envisioned to be away from equalizing, with the deviations differing in different topologies, due to the various paths used to compute the voltage.

The input port impedance characterization results for the LC-filled SL phase shifter are plotted in Fig. 1. Looking more closely at the  $W_{core}$  of 90  $\mu\text{m}$  (wherein the  $50 \Omega$  impedance matching is obtained for the  $Z_{pi}$  metric), a 2.015  $\Omega$  deviation is evidenced amidst the three methods.

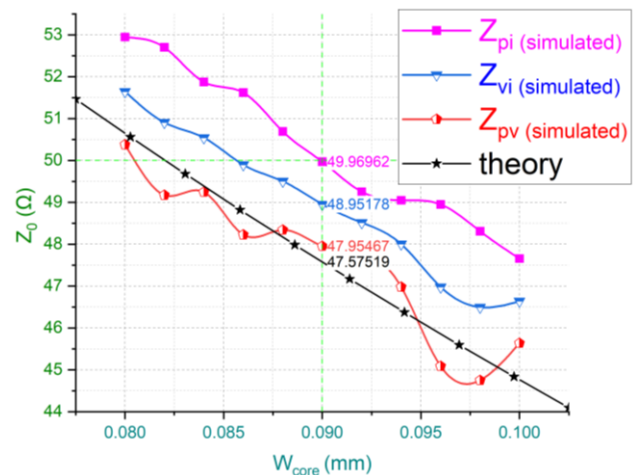


Fig. 1. Full-wave FEM characterization and theoretical benchmark of  $Z$  for LC-filled strip line phase shifter at 60 GHz, with nematic LC fully biased at  $Dk=3.3$  (saturated state).

A similar working principle is applied to the LC-filled IMSL phase shifter at the maximally biased LC state. Here the air-box radiating boundary (as per the real-world practice for a device without installing metal enclosures) applies as per our latest work analyzed from the angle of device packaging and symmetry [9]. As observed from Fig. 2, the

computed  $Z$  deviations of up to  $2.496 \Omega$  amidst the three approaches are acquired and illustrated at 60 GHz, parameterizing  $W_{\text{core}}$  at which  $Z_{\text{pi}}$  of  $50 \Omega$  is obtained at  $W_{\text{core}}$  of  $0.1616 \text{ mm}$ . The results of various  $Z$  for the LC-filled coaxial one are shown in Fig. 3, with the maximum deviation (at  $Z_{\text{pi}}$  of  $50 \Omega$ ) limited to less than  $0.254 \Omega$  amidst the three methods as well as the theoretical approach.

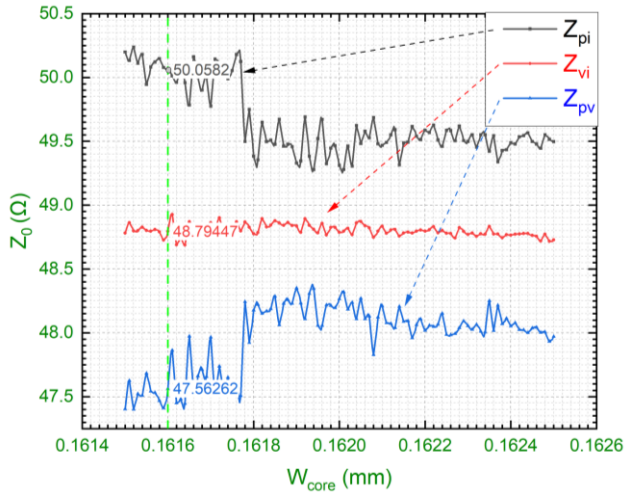


Fig. 2. Full-wave FEM characterization of  $Z$  for LC-filled IMSL phase shifter at 60 GHz, with nematic LC fully biased at  $Dk=3.3$  (saturated state).

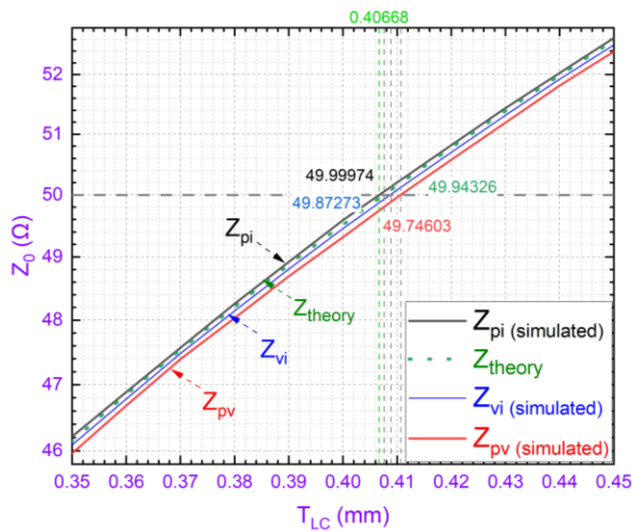


Fig. 3. Full-wave FEM characterization and theoretical benchmark of  $Z$  for LC-filled coaxial phase shifter at 60 GHz, with nematic LC fully biased at  $Dk=3.3$  (saturated state).

If we replace the LC material with a new one that exhibits the maximally achievable  $Dk$  of  $3.68$  at the saturated bias, the conducted  $50 \Omega$  search for the  $W_{\text{core}}$  is shown in Fig. 4. Comparing the results of Fig. 4 with those in Fig. 2, the increased  $Dk$  of the filled dielectric tends to reduce the  $Z$ , and hence relatively lower values of  $W_{\text{core}}$  are evidenced (in Fig. 4) for the  $50 \Omega$  match, i.e.,  $0.145 \text{ mm}$  here ( $<0.1616 \text{ mm}$  for IMSL with  $Dk$  of  $3.3$  in maximum). This well agrees with the physics of the tunable dielectrics. At  $W_{\text{core}}$  of  $0.145 \text{ mm}$  ( $50 \Omega$  for  $Z_{\text{pi}}$ ), the maximum deviation amidst the three approaches is within  $0.6027 \Omega$ , i.e., far lower than that of the LC IMSL design with  $Dk=3.3$ . Note that the results shown for both the LC IMSL designs ( $Dk=3.3$  at Fig. 2, and  $Dk=3.68$  at Fig. 4) are obtained by simulations in a unified

computational framework (i.e., following the same regulation of the adaptive meshing and convergence).

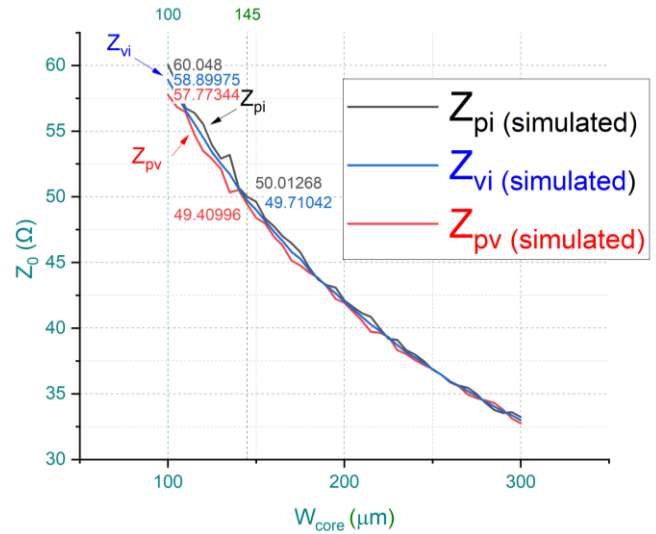


Fig. 4. Full-wave FEM characterization of  $Z$  for an LC-filled IMSL phase shifter at 60 GHz, with nematic LC fully biased at  $Dk=3.68$  (saturated state of a new grade of nematic LC material).

In summary, an electromagnetically closed structure (e.g., coaxial) is likely to exhibit the lowest deviation in  $Z$  amidst the diverse characterization methods of  $Z_{\text{pi}}$ ,  $Z_{\text{pv}}$ , and  $Z_{\text{vi}}$ . For the same geometry type (e.g., the semi-open IMSL), using the LC material with a higher achievable  $Dk$  tends mitigating this discrepancy between  $Z$  using diverse characterization approaches.

Interestingly, comparing our results (insights) derived from our LC-based transmission lines (planar IMSL and non-planar, i.e., coaxial and SL) with previous people's analysis into waveguides [21], the key pattern is reshuffled, i.e.,  $Z_{\text{pi}} > Z_{\text{vi}} > Z_{\text{pv}}$  (derived in this work on transmission lines) as compared with  $Z_{\text{pv}} > Z_{\text{vi}} > Z_{\text{pi}}$  (derived by [21] on rectangular waveguides WR-90 and WR-42, as well as circular waveguides). The comparison is qualitatively summarized in Table I below. More specifically, the computed characteristic impedances of both transmission lines and waveguides exhibit the averaged (more precisely, intermediate) level when using the voltage-current approach ( $Z_{\text{vi}}$ ) to calculate.

TABLE I  
RESULTS COMPARISON OF CALCULATION-APPROACH-DEPENDENT IMPEDANCE CHARACTERIZATIONS

Z Status	This work on three transmission lines filled with LC	Rectangular and circular waveguides [21]
Highest	$Z_{\text{pi}}$	$Z_{\text{pv}}$
Intermediate	$Z_{\text{vi}}$	$Z_{\text{vi}}$
Lowest	$Z_{\text{pv}}$	$Z_{\text{pi}}$

Based on the foundational results and observations obtained above on the impedance characterization for LC-embedded transmission line design, an LC-filled coaxial phase shifter is continued to be investigated in a case study upscaling from 60 GHz to 0.3 THz (i.e., 300 GHz), as elaborated in section III.

III. CONSERVATIVENESS ASSESSMENT OF GUARD BAND ALLOWANCE FOR LC TERAHERTZ COAXIAL PHASE SHIFTERS

Our foundational works on LC coaxial phase shifter at 300 GHz [22][23] feature the extensiveness in terms of offering a differentiated methodology and purpose of existing studies, such as coaxial transmission line design, suppression of higher-order modes, constitutive loss quantification, leveraging analytical and simulation-based approaches, primarily aimed at addressing the varying levels of tension between THz frequency challenges and protocols. One of our unanswered questions, however, is the conservativeness of the guarding band boundary (25% defined in our first documented design [22]), and the resultant phase shift compromise (to be further elaborated in this work).

A. Perturbing Guarding Band and Benchmark Results

To further the previous 300 GHz critical structure identification (TE<sub>11</sub> mode cutoff with 25% guarding band applied, i.e., pushing the cutoff frequency from the 300 GHz upwards to 375 GHz), the solutions of LC thicknesses and core line diameters for the filled LC's dielectric constant (Dk) from 1 to 5 are plotted in Fig. 5.

By investigating the redundancy level that is perturbative from 0% (no allowance) to 50% by design, the corresponding critical structural geometry of the 300 GHz operation device is derived mathematically (as per the assumptions detailed in [22]) from the LC thickness of 0.1148 mm and the core line diameter of 0.07688 mm (0% allowance) to the LC thickness of 0.07653 mm and the core line diameter of 0.05125 mm (50% allowance), all based on the 50 Ω matched at the LC isotropic state (Dk=2.754).

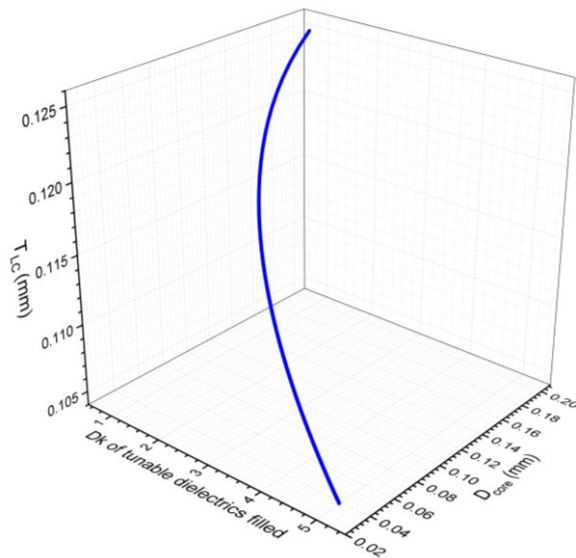


Fig. 5. Analytical solutions of LC-filled coaxial critical structure sizes for TE<sub>11</sub> mode-cutoff at 375 GHz (25% allowance reserved for 300 GHz operation, critical geometry identified based on critical wavelength formulation proposed in [22]).

Accordingly, the maximum differential phase shifts (Fig. 6), maximum insertion losses (Fig. 7), and hence the resulting figure-of-merit (FoM, see Fig. 8) are quantified and compared with the analytical results (scaled from 60 GHz to 300 GHz based on electronics theory). All the scattering parameters are renormalized to 50 Ω for emulating the connectors' effect in practice. In accordance with the 60 GHz characterization results [6] for the LC-filled coaxial phase

shifter's FoM (102.46°/dB) and the phase shifting capability per unit length and per unit gigahertz (1.884°/dB/GHz), the theoretically predicted differential phase shift that can be achieved at 300 GHz should be 565.327°, whereas the simulated result here gives 206.087° as confirmed by the semi-theoretical result of 206.6812° (for the 0% allowance one), i.e., a 63.5% decline is evidenced (benchmarked with the 565.327° prediction by scaling from 60 GHz to 300 GHz). This also leads to a 64.7% slump in the claimed FoM (from 102.46°/dB at 60 GHz to 36.16894°/dB at 300 GHz).

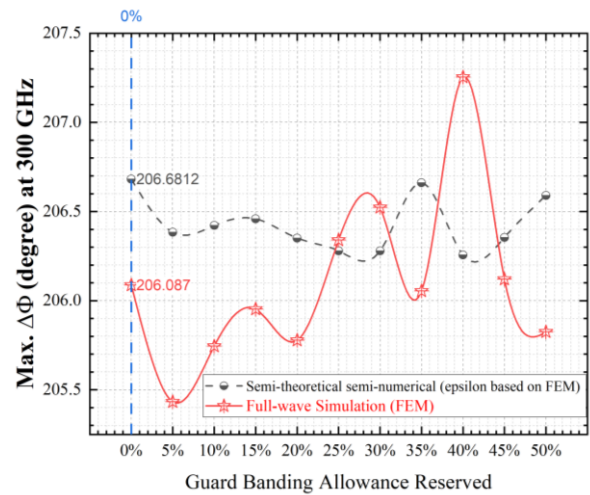


Fig. 6. FEM-based full-wave simulated maximum differential phase shift of 300 GHz LC coaxial phase shifter designs based on guard band perturbing from 50% (1.5 times the operational frequency) to 0% (no reservation), number of modes set as 1 on both ports to enforce single-mode-only input and observation (results benchmarked by semi-theoretical semi-numerical study incorporating effective permittivity computed for coaxial transmission line at extreme tuning states of LC).

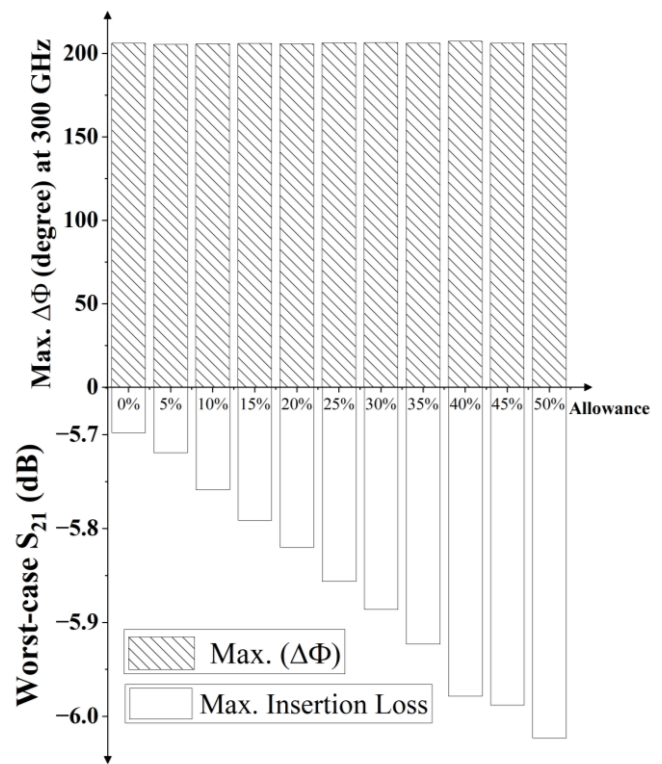


Fig. 7. FEM-based full-wave simulated performance of maximum differential phase shift and maximum insertion loss of 300 GHz LC coaxial phase shifter designs based on guard band perturbing from 50% (1.5 times the operational frequency) to 0% (no reservation), number of modes set as 1 on both ports to enforce single-mode-only input and characterization.

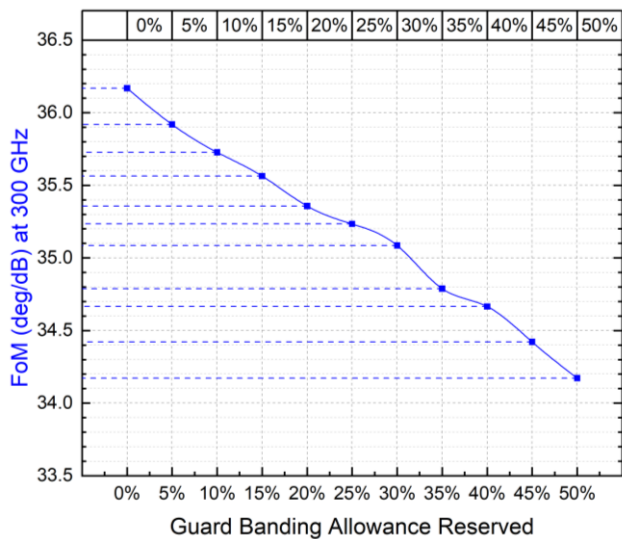


Fig. 8. FEM-based full-wave simulated FoM of 300 GHz LC coaxial phase shifter designs based on guard band perturbing from 50% (1.5 times the operational frequency) to 0% (no reservation), number of modes set as 1 on both ports to enforce single-mode-only input and observation.

Comprehensively, although the decrease in FoM is partially due to the surge in the insertion loss, which has well been explained in our loss decomposition study [6][22], the phase shifting degradation has yet to be interpretable from the mmW electronics theory. From the phase-shifting gap observed between the theoretically scalable electronics and computational electromagnetics, we arguably predict the existence of higher-order modes that occur at the THz range. These parasitic modes not only dissipate the transmission power of the fundamental coaxial TEM mode, but also reduce the effectiveness of the tunable dielectrics in reconfiguring the phase of interest.

B. Application Scopes at THz

Like inkjets are for more than printing [24], terahertz (THz) is for more than imaging, it can build high-data-rate communications [25] and much more [22]. Ultra-high-speed wireless communications, technically possible at sub-millimeter-wave (sub-mmW) and THz frequencies, are essential for the development of next-generation networks (such as 5G and beyond) [4], targeting not only ground applications (e.g., cloud XR, data center, indoor hotspots), but also space (e.g., intersatellite communication [7], spaceship communication), and even chip-to-chip communication [26]. Therefore, the scientific and technology community will gain a great deal from any research that presents new ideas or even enhances current technologies.

Among the tsunami of new technologies and research efforts, liquid crystal (LC) enabled reconfigurable components have been gaining traction in the recent two decades [5] due to their continuous tunability (i.e., high-resolution tuning) when exposed to a low-power-consuming voltage driving field [27] in place of power-hungry magnetic tuning [28]. The tuning functionality can be multi-purpose by design, e.g., phase [22][23], amplitude [7], frequency [29], polarization [30]. Relevant demos have been evidenced in the realms of microwave [7], mmW [31], and catching on to THz [32] recently, driving new waves of fast-growth innovation and companies spun

out. By way of illustration, Fig. 9 below depicts the wide scopes of applications in astrophysics, detection, sensing, biomedical, farming, and even for the cultural heritage protection [33].

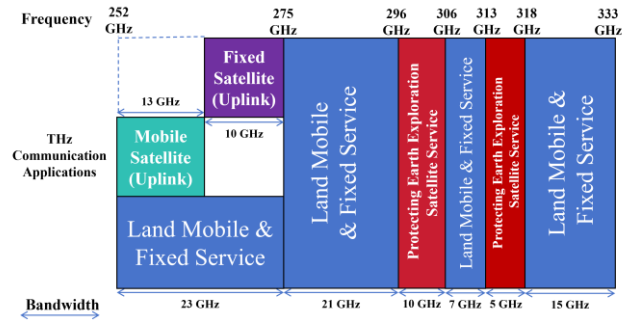


Fig. 9. A sketch of potential applications of LC-filled transmission line-based phase shifters in planned terahertz communication spectrum from 252 GHz to 333 GHz.

IV. DISCUSSION AND CONCLUDING REMARKS

A. Summary of New Contributions and Implications

At the outset of the paper, this work contributes a unified impedance characterization framework by benchmarking three methods, i.e.,  $Z_{pi}$  (power-current),  $Z_{vi}$  (voltage-current), and  $Z_{pv}$  (power voltage) for three distinct types of phase-variable transmission lines, i.e., inverted microstrip line, strip line, and coaxial line, all filled with highly anisotropic nematic LCs embedded as electronically tunable media. While the three topologies all exhibit two conductors, the main difference is de facto the existence of non-tunable dielectrics or not, and thus the impact from the mmW power shared with them.

First, the 60 GHz computational benchmark results in this work validate that the  $Z_{pi} > Z_{vi} > Z_{pv}$  phenomenon applies for the three transmission-line topologies but varies in the deviation levels that are a function of the geometry aspect ratio of core line to LC layer thickness, as well as the permittivity ratio of the tunable (LC) to non-tunable dielectrics (for IMSL only). Based on identical LC permittivity at 60 GHz, the maximum deviation amidst the three impedances of IMSL is 2.8  $\Omega$ , while the strip line exhibits 2.01  $\Omega$ , and it drops to 0.4  $\Omega$  for the coaxial one.

Expanding on the implications of these results, a more sophisticated comprehension of impedance properties and deviation patterns is crucial for improving the performance and design of mmW reconfigurable components that use LC-based transmission lines. This will lead to increased adaptability and more precise performance prediction in a variety of applications, including radar systems [34][35], 5G/6G wireless communication networks and high-precision detection [36].

Another implication from the applied study reported in section III is the polyimide (PI)-free liquid crystal (LC) phase shifter, which has the advantage of quicker tuning response than conventional PI-rubbed alignment-based devices. One of the technical realization possibilities in terahertz is structuring the LC layer coaxially, thus reconfiguring between the isotropic LC status (no PI anchoring required) and the saturated LC status (low-frequency voltage applied to the core line and outer conductor for dipole reorientations). While the phase shifting and dissipative loss were

numerically predicted at 0.3 THz and compared with the 60 GHz design in the millimeter-wave regime laying out in our first feasibility study, one unanswered question is the conservativeness of the TE11 cutoff guard band proposal we conceptualized for the 0.3 THz LC coaxial phase shifter designs.

Specifically, a 25% guarding band was reserved away from the TE11 mode cutoff frequency, resulting in a reduced device footprint, tighter tolerances in manufacturing, and hence a surge in the overall costs. The guard banding redundancy level is thereby reinvestigated in this work by parametrizing from 50% (i.e., the 0.3 THz TEM operated device is designed as per the 0.45 THz TE11 cutoff standard) downwards to 0% (i.e., no guard banding protection), figuring out the updated patterns of the phase shifts (differential) and forward transmission coefficients (insertion loss) to answer the question concerning the possibility of relaxing the conservative assumption for staying away from the vulnerability of higher-order modes for a reduced cost and enhanced manufacturability. Results reveal that the full-wave scalability theory from microwave electronics fails to interpret the significant degradations of phase shifting capability per unit length and per unit frequency (by 63.5%), as well as the figure-of-merit (decline by 64.7%) in the 0.3 THz designs (as compared with the 60 GHz ones), for which photonics is envisaged to decipher the struggled higher-order-mode quantification problem.

*B. Scope for Future Research*

In future work, we will present a comprehensive analysis and results, encompassing not only the operational case for the lowest dielectric constant (Dk) tuning state with liquid crystal (LC) but also the scenarios without LC. These include pre-injection and post-disposal states, where the cavity is dielectrically filled with air by default, as illustrated in Fig. 10. To enhance accuracy, we will introduce LC-specific closed-form expressions along with discrete air-filled states (Dk of 1.00059), replacing the traditional formulas that account solely for the LC Dk tuning range. Consequently, the device's maximum operational impedance, inclusive of pre-commissioned and decommissioned states, is expected to increase by a factor of 1.659, assuming the lowest operational Dk of LC is 2.754, as reported in [6] and [22].

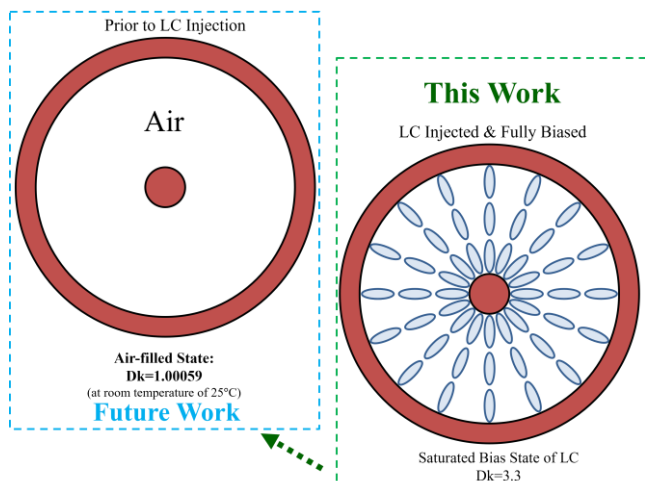


Fig. 10. A schematic representation of air-filled dielectric state in LC-enabled coaxial phase shifter (prior to LC injection or post-disposal of LC), to be incorporated into the analysis of device's various operational states in future work.

For the applied study into the 0.3 THz LC-filled coaxial phase shifter, future work underway is committing the ideas towards unifying the insertion loss degradation (observed in the past) and the phase shift compromise (raised in the current work) from mmW to THz, igniting the ambition of achieving an operational THz coaxial LC phase shifter rollout without sacrificing the phase-shifting scalability. Leveraging state-of-the-art LC photonics at THz [37] and beyond [38] both computationally and experimentally will be attempted to probe and validate the theoretical scalability limit of LC-combined mmW electronics [39] towards THz [40] and optical wavelengths [41].

Specifically, new paradigms (addressing the computational vulnerabilities as spotted in [42]) and algorithms (beyond conventional FEM [43][44][45]) will be proposed to complement the full-wave theoretically scalable electronics in addressing the inferior characterization accuracy problem in the THz regime.

REFERENCES

- [1] Li J, and Chu D, "Liquid crystal-based enclosed coplanar waveguide phase shifter for 54–66 GHz applications," *Crystals*, vol. 9, no. 12, 650, 2019.
- [2] Li J, "Millimetre-wave beam steering with analog-resolution and minimised distortion based on liquid crystals tunable delay lines with enhanced signal-to-noise ratios," *Proceedings of SPIE, Millimetre Wave and Terahertz Sensors and Technology XIII*, vol. 11541, pp 115410H, 2020.
- [3] Hansen C, "WiGiG: Multi-gigabit wireless communications in the 60 GHz band," *IEEE Wireless Communications*, vol. 18, no. 6, pp6-7, 2011.
- [4] Li J, "From Liquid Crystal on Silicon and Liquid Crystal Reflectarray to Reconfigurable Intelligent Surfaces for Post-5G Networks," *Applied Sciences*, vol. 13, no. 13, 7407, 2023.
- [5] Li J, "Challenges and Opportunities for Nematic Liquid Crystals in Radio Frequency and Beyond," *Crystals*, vol. 12, 5, 632, 2022.
- [6] Li J, and Li H, "Liquid Crystal-Filled 60 GHz Coaxially Structured Phase Shifter Design and Simulation with Enhanced Figure of Merit by Novel Permittivity-Dependent Impedance Matching," *Electronics*, vol. 13, no. 3, 626, 2024.
- [7] Li J, "All-optically Controlled Microwave Analog Phase Shifter with Insertion Losses Balancing," *Engineering Letters*, vol. 28, no. 3, pp663-667, 2020.
- [8] Li J, "Towards 76-81 GHz Scalable Phase Shifting by Folded Dual-strip Shielded Coplanar Waveguide with Liquid Crystals," *Annals of Emerging Technologies in Computing*, vol. 5, no. 4, pp14-22, 2021.
- [9] Li J, and Li H, "Symmetry Implications of a 60 GHz Inverted Microstrip Line Phase Shifter with Nematic Liquid Crystals in Diverse Packaging Boundary Conditions," *Symmetry*, vol. 16, no. 7, 798, 2024.
- [10] Li J, and Li H, "Impedance Characterization for Liquid Crystal Tunable Coaxial Transmission Lines at 60 GHz," *Proceedings of the 2023 Cross Strait Radio Science and Wireless Technology Conference*, pp1-3, 2024.
- [11] Edwards T, and Steer M, "Stripline Design," *Foundations for Microstrip Circuit Design*, pp369383, 2016.
- [12] Lee G, Mohyuddin W, Kumar S, Choi H, and Kim K, "Compact Wideband Coplanar Stripline-to-Microstrip Line Transition Using a Bended Structure on a Two-Layered Substrate," *Electronics*, vol. 10, no. 11, 1272, 2021.
- [13] Ghimire J, Khan D, and Choi D, "Microstrip to Slot-Line-Fed Microstrip Patch Antenna with Radiation Pattern Diversity for X-Band Application," *Electronics*, vol. 12, no. 17, 3672, 2023.
- [14] Kubacki R, Czyżewski M, and Laskowski D, "Minkowski Island and Crossbar Fractal Microstrip Antennas for Broadband Applications," *Applied Sciences*, vol. 8, no. 3, 334, 2018.
- [15] Ibrahim L, Abbas Z, Azis R, Ibrahim N, and Abd R, "The Effect of MWCNTs Filler on the Absorbing Properties of OPEFB/PLA Composites Using Microstrip Line at Microwave Frequency," *Materials*, vol. 13, no. 20, 4581, 2020.
- [16] Radha, S, Choi S, Lee J, Oh J, Cho I, and Yoon I, "Ferrite-Loaded Inverted Microstrip Line-Based Artificial Magnetic Conductor for the Magnetic Shielding Applications of a Wireless Power Transfer System," *Applied Sciences*, vol. 13, no. 18, 10523, 2023.

- [17] Musa S, and Sadiku M, "Modeling of shielded, suspended and inverted, microstrip lines," Proceedings of the IEEE SoutheastCon 2008, pp309-313, 2008.
- [18] Li J, and Li H, "Computationally Sampling Surface and Volume Current Densities of Liquid Crystal Non-Planar Phase Shifters for Low-Loss 5G IoT and 6G AIoT," Proceedings of the 2024 IEEE International Conference on Omni-layer Intelligent Systems, pp1-6, 2024.
- [19] Li J, and Li H, "Frequency Ripples Reduction in Differential Delay Time of Liquid Crystals Coaxial Delay Lines," Proceedings of the 2024 IEEE INC-USNC-URSI Radio Science Meeting (Joint with AP-S Symposium), pp154-155, 2024.
- [20] Li J, and Li H, "Navigating Aspect Ratio Effects in Response Time Challenges of Liquid Crystal Coaxial Phase Shifters for Next-Generation mmW Communications," Proceedings of the IEEE 11th International Conference on Wireless Networks and Mobile Communications, pp1-5, 2024.
- [21] Herhil Y, Piltyay S, Bulashenko A, and Bulashenko O, "Characteristic Impedances of Rectangular and Circular Waveguides for Fundamental Modes," Proceedings of the 2021 IEEE 3rd Ukraine Conference on Electrical and Computer Engineering, pp46-51, 2021.
- [22] Li J, and Li H, "Modeling 0.3 THz Coaxial Single-Mode Phase Shifter Designs in Liquid Crystals with Constitutive Loss Quantifications," Crystals, vol. 14, no. 4, 364, 2024.
- [23] Li J, and Li H, "Liquid Crystal Coaxial Phase Shifter Designs at 0.3 THz," Springer Proceedings in Physics, pp147-151, 2024.
- [24] Barth P, and Field L, "Inkjets Are for More Than Just Printing: They can Build DNA Arrays, 3D Structures, and Much More," IEEE Spectrum, vol. 61, no. 4, pp32-37, 2024.
- [25] Fujishima M, "Future of 300 GHz band wireless communications and their enabler, CMOS transceiver technologies," Japanese Journal of Applied Physics, vol. 60, no. SB0803, 2021.
- [26] Elkarkraoui T, Ahmadi M, and Naeini S, "Terahertz Band Interconnect Architecture for Future Chip-to-Chip Wireless Communication," Proceedings of the 45th International Conference on Infrared, Millimeter, and Terahertz Waves, pp1-2, 2020.
- [27] Nishimura S, Masuyama S, Shimizu G, Chen C, Ichibayashi T, and Watanabe J, "Lowering of Electrostatic Actuator Driving Voltage and Increasing Generated Force Using Spontaneous Polarization of Ferroelectric Nematic Liquid Crystals," Advanced Physics Research, vol. 1, no. 1, 2200017, 2022.
- [28] Hahsler M, Nadasi G, Feneberg M, Marino S, Giesselmann F, Behrens S, and Eremin A, "Magnetic Tilting in Nematic Liquid Crystals Driven by Self-Assembly," Advanced Functional Materials. vol. 31, no. 31, 2101847, 2021.
- [29] Humar M, Ravnik M, Pajk S, and Musevic I, "Electrically tunable liquid crystal optical microresonators," Nature Photonics, vol. 3, pp 595-600, 2009.
- [30] Doumanis E, Goussetis G, Dickie R, Cahill R, Baine P, Bain M, Fusco V, Encinar J, and Toso G, "Electronically Reconfigurable Liquid Crystal Based Mm-Wave Polarization Converter," IEEE Transactions on Antennas and Propagation, vol. 62, no. 4, pp2302-2307, 2014.
- [31] Li J, "60 GHz 0-360° Passive Analog Delay Line in Liquid Crystal Technology based on a Novel Conductor-backed Fully-enclosed Coplanar Waveguide," Proceedings of the 2022 IEEE 72nd Electronic Components and Technology Conference, pp. 1841-1846, 2022.
- [32] Fedotov V, "Phase control of terahertz waves moves on chip," Nature Photonics, vol. 15, pp715-716, 2021.
- [33] Cosentino A, "Terahertz and Cultural Heritage Science: Examination of Art and Archaeology," Technologies, vol. 4, no. 1, 6, 2016.
- [34] Dill S, Peichl M, Schreiber E, and Anglberger H, "Improved characterization of scenes with a combination of MMW radar and radiometer information," Proceedings of SPIE, vol. 10189, pp1018907, 2017.
- [35] Korn B, Doehler H, and Hecker P, "MMW-radar-based navigation: solutions to the vertical position problem," Proceedings of SPIE, vol. 4023, pp29-37, 2000.
- [36] Berrios J, Chen D, Schlegel A, Vakalis S, and Nanzer J, "Incoherent millimeter-wave imaging using 5G communications signals of opportunity for detection of cracks in building materials," Proceedings of SPIE, vol. 12535, pp125350J, 2023.
- [37] Yu H, Wang H, Wang Q, Ge S, and Hu W, "Liquid Crystal-Tuned Planar Optics in Terahertz Range," Applied Sciences, vol. 13, no. 3, 1428, 2023.
- [38] Dierking I, "Progress in liquid crystal science and technology," Liquid Crystals Today, vol. 22, no. 3, pp62-63, 2013.
- [39] Li J, and Li H, "Effective Dielectric Constant Benchmark of 60 GHz Liquid Crystal-Filled Coaxial Delay Line," Proceedings of the 2024 IEEE International Conference on Computational Electromagnetics, pp1-3, 2024.
- [40] Ung B, Liu X, Parrott E, Srivastava A, Park H, and Chigrinov V, "Towards a Rapid Terahertz Liquid Crystal Phase Shifter: Terahertz In-Plane and Terahertz Out-Plane (TIP-TOP) Switching," IEEE Transactions on Terahertz Science and Technology, vol. 8, no. 2, pp209-214, 2018.
- [41] Harris S, "Liquid crystal optical phased arrays: Practical issues and applications," Proceedings of the 15th Annual Meeting of the IEEE Lasers and Electro-Optics Society, pp520-521, 2022.
- [42] Li J, and Li H, "Assessing Vulnerabilities in Line Length Parameterization and the Per-Unit-Length Paradigm for Phase Modulation and Figure-of-Merit Evaluation in 60 GHz Liquid Crystal Phase Shifters," Symmetry, vol. 16, no. 10, 1261, 2024.
- [43] Li J, and Li H, "Finite-element Adaptive Meshing Statistics of Liquid Crystal Coaxial Phase Shifters for mmW Electronics and THz Photonics Beyond Display: A Comparative Study," Photonics Letters of Poland, vol. 16, no. 3, pp40-42, 2024.
- [44] Parra S, Pappalardo C, Estrada O, and Guida D, "Finite Element based Redesign and Optimization of Aircraft Structural Components using Composite Materials," IAENG International Journal of Applied Mathematics, vol. 50, no. 4, pp860-877, 2020.
- [45] Li J, and Li H, "Susceptibility to Low-Frequency Breakdown in Full-Wave Models of Liquid Crystal-Coaxially-Filled Noise-Shielded Analog Phase Shifters," Electronics, vol. 13, no. 23, 4792, 2024.

**Jinfeng Li** (M'20) is an Engineering Scientist, a specialist in novel reconfigurable RF devices, as well as an authority on liquid crystals-based microwave and millimetre-wave technology. He received the B.Eng. degree (1st class) in electrical and electronics engineering from the University of Birmingham and Huazhong University of Science & Technology, in 2013, the MPhil degree in nuclear energy from the University of Cambridge, in 2014, and the Ph.D. degree in liquid crystals microwave and millimetre-wave electronics engineering from the University of Cambridge, in 2019.

From 2019, he joined the University of Southampton as a research fellow, Imperial College London as a visiting research fellow, and Nuclear Futures Institute (Bangor University) as a research associate. He is currently an Assistant Professor with Beijing Key Laboratory of Millimeter Wave and Terahertz Technology at Beijing Institute of Technology. In the past ten years, his research experiences include (1) microwave and millimetre-wave beam steering and tunable devices based on liquid crystals for 5G/6G, inter-satellite communications, and radio astronomical instrumentation; (2) wireless surface acoustic wave sensors antenna array for monitoring the structural integrity of LNG tanks; (3) light water reactor thermal hydraulics facility and instrumentation development in North Wales; (4) optical fiber based multi-phase flow characterization; (5) computational modelling of nuclear reactor core using Monte Carlo and deterministic methods for nuclear energy policy decision-making; (6) motor drives of multilevel multicell inverters for fuel economy and sustainable cities; (7) application security and sentiment analysis of big data for stock market forecasting; (8) contact tracing and health informatics for COVID-19 (cited by PNAS and Lancet Public Health). He has edited three books, authored or co-authored over 70 journal and conference papers.

Prof. Li was a recipient of the IET Award, the AP Jarvis Prize (highest final-year-project honour in University of Birmingham), the AETIC Highly Cited Article Award 2023, and three Best Paper Awards at IEEE, IOP and IET conferences, respectively. He was a Cambridge Trust Scholar, Speaker at IEEE AP-S/URSI 2024 and the 50th & 46th European Microwave Conferences, Emerging Technologist with Barclays UK, Editorial Board member of three Science Citation Index journals, TPC and Session Chair of seven IEEE conferences, including IEEE ISAP (27th International Symposium on Antennas and Propagation), IEEE 15th International Conference on Microwave and Millimeter Wave Technology (ICMMT 2023), IEEE 10th International Conference on Control, Decision and Information Technologies (CoDIT 2024), IEEE COINS 2024, IEEE SNAMS 2019, IEEE VCC 2024, and 5th China and International Young Scientist Terahertz Conference etc. He was elected Senior Member of the China Institute of Communications (CIC), Top 1% Reviewer on Publons (Web of Science), Reviewing Expert for the China Academic Degrees and Graduate Education Development Center, Grants Reviewer for the National Natural Science Foundation of China (NSFC), Newton Prize (£1m fund) reviewer for the UK National Commission for UNESCO, and Grants Reviewer for the Health and Social Care Delivery Research (HSDR) fund from National Institute for Health Research (NIHR), UK. Prof. Li is also a Concert Pianist and Composer with more than 20 piano recitals across China and the UK (2004 - now). Prof. Li was elected National-level Young Talent in 2023. He teaches three undergraduate modules including (1) States of the Arts in Liquid Crystals Millimeter-wave Technology for 6G; (2) Frontiers and Progress of Electrical and Computer Engineering; and (3) Frontiers of

Electronic Science and Technology. He and his student won the Best Paper Award at IET GEN-CITY 2024.

**Haorong Li** is pursuing a postgraduate degree in microwave and terahertz engineering at Beijing Institute of Technology under the supervision of Prof. Jinfeng Li who leads the Liquid Crystal Millimeter-wave Technology Group. Haorong received the Special Scholarship from the School of Integrated Circuits and Electronics and was awarded the Excellent Postgraduate Student title at Beijing Institute of Technology in 2024. He won the Best Paper Award (Student) at IET International Conference on Green Energy, Computing and Intelligent Technology (GEN-CITY 2024).